Endoscopic pulsed digital holography for 3D measurements

A. Tonatiuh Saucedo, Fernando Mendoza Santoyo, Manuel De la Torre-Ibarra

Centro de Investigaciones en Optica, A.C., Loma del Bosque 115, Leon, Guanajuato, Mexico 37150

Giancarlo Pedrini and Wolfgang Osten

Institut für Technische Optik, Universität Stuttgart, Pfaffenwaldring 9, D-70569 Stuttgart, Germany.
tsaucedo@cio.mx

Abstract: A rigid endoscope and three different object illumination source positions are used in pulsed digital holography to measure the three orthogonal displacement components from hidden areas of a harmonically vibrating metallic cylinder. In order to obtain simultaneous 3D information from the optical set up, it is necessary to match the optical paths of each of the reference object beam pairs, but to incoherently mismatch the three reference object beam pairs, such that three pulsed digital holograms are incoherently recorded within a single frame of the CCD sensor. The phase difference is obtained using the Fourier method and by subtracting two digital holograms captured for two different object positions.

OCIS codes: (090.2880) Holographic interferometry; (170.2150) Endoscopic imaging; (120.4630) Optical inspection; (120.5050) Phase measurement

References and links

1. D. Hadbawnik,"Holographische endoskopie," Optik **45**, 21-38 (1976).
2. H. I. Bjelkhagen, M. D. Friedman and M. Epstein, "Holographic high resolution endoscopy through optical fiber," Proc. Laser Inst. Am. **64**, 94-103 (1988).
3. M. Yonemura, T. Nishisaka, and H. Machida, "Endoscopic hologram interferometry using fiber optics," Appl. Opt. **20**, 1664-1667 (1981).
4. B. Kemper, D. Dirksen, W. Avenhaus, A. Merker, and G. Von Bally, " Endoscopic double pulse electronic speckle pattern interferometer for technical and medical intracavity inspection," Appl. Opt. **39**, 3899-3905 (1999).
5. G. Pedrini, S. Schedin, and H. J. Tiziani, "Use of endoscopes in pulsed digital holographic interferometry," in Optical Measurement System for Industrial Inspection II: Applications in productions Engineering, R. Holfling, W. Jupter and M. Kujawinska, eds. Proc. SPIE **4399**, 1-8 (2001).
6. O. Coquoz, R. Conde, R. Taleblou, and C. Depeursinge, " Performance of endoscopy holography with a multicore optical fiber," Appl. Opt. **34**, 7186-7193 (1995).
7. C. M. Vest, *Holography Interferometry*, (Wyle, New York, 1979).
8. Staffan Schedin, G. Pedrini, H. J. Tiziani, and Fernando Mendoza Santoyo, "Simultaneous three-dimensional dynamic deformation measurement with pulsed digital holography," Appl. Opt. **38**, 7056-7062 (1999).
9. G. Pedrini and I, Alexeenko,"Miniaturized optical system based on digital holography," Sixth International Conference on Vibration Measurements by Laser Techniques: Advances and Applications, Procceeding of SPIE, **5503**, 423-498 (2004).
10. Ervin Kolenovic, Wolfgang Osten, Reiner Klattenhoff, Songcan Lai, Chritoph Von Kopylow, and Werner Juptner. "Miniaturized digital holography sensor for distal three-dimensional endoscopy," Appl. Opt. **42**, 5167-5172 (2003).

1. Introduction

Non contact full field optical techniques such as speckle and holographic interferometry are being developed in order to apply them to the study of displacements, crack detection or any other type of defects that are in areas hidden within an object, superficially or within its walls. Both techniques have been well received in the past as a solution to 3D measure static and

#9861 - $15.00 USD Received 5 December 2005; revised 30 January 2006; accepted 1 February 2006

dynamic events from object areas easily imaged and in many types of environmental conditions. A drawback to date has been the gaining of access to hidden areas, mainly because the imaging device, e.g., an endoscope, did not have enough image resolution and thus both techniques did not render significant results [1]. Besides, the interferogram analysis for speckle and holography had to be done using data stored on photographic and holographic films, respectively [1-3]. Good quality image endoscopes and high resolution CCD sensors appeared recently, making it possible to design systems capable of obtaining out-of-plane displacements [4-6]. Non endoscopic pulsed speckle and digital holographic interferometric systems have been used in the past to measure displacements along all three perpendicular coordinate axes x, y and z. The optical set up relied on the object surface being illumined from three diverging sources located at three arbitrary, but known, positions [7]. The majority of those systems acquire the information sequentially, meaning that the experiment has to be repeated several times. There are however, occasions in which the experiment cannot be repeated and then a system was designed to simultaneously acquire in a single CCD frame the three orthogonal displacement components [8] from the easily seen surface of a harmonically vibrating object.

The aim of the research work reported here was to design a pulsed digital holography system that incorporates a high image quality rigid endoscope that carries on it three multi mode optical fibers used to illuminate and hence simultaneously interrogate in 3D hidden object areas. Results from the three orthogonal displacements x, y and z are presented from the inner surface of a metallic cylinder subjected to harmonic vibrations. These three components may be individually studied and combined to get useful information as the tangential and normal, to the surface, object displacements.

2. **3-D Evaluation**

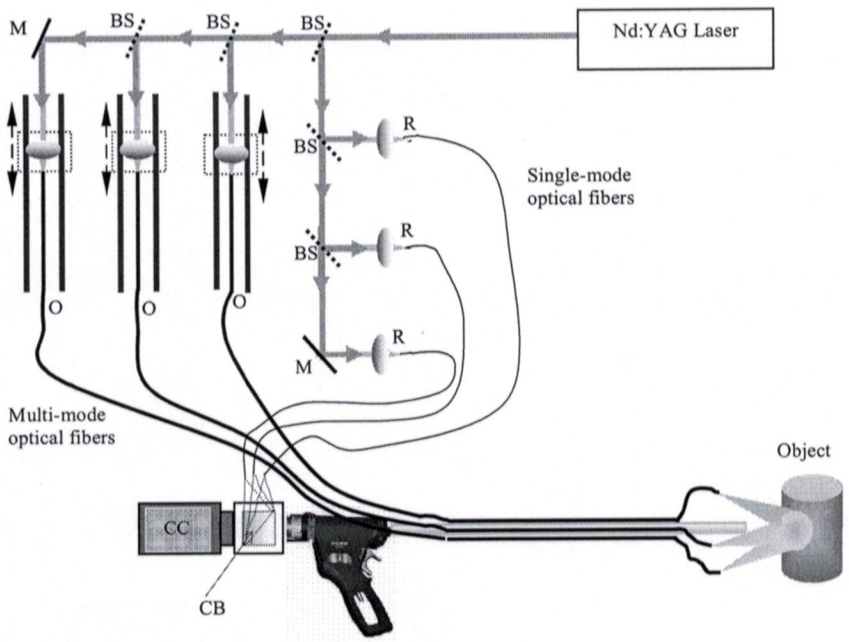

Fig. 1 .Experimental set up for the 3D endoscopic pulsed digital holography with simultaneous recording of three digital holograms. BS, Beam splitters; CB, Cube beam splitters; M, mirrors; O, object illumination beams; R reference beams.

#9861 - $15.00 USD
Received 5 December 2005; revised 30 January 2006; accepted 1 February 2006

In order to incoherently store in a single CCD frame the information from the three reference object beam pairs it is necessary to make their respective optical path lengths different by at least the laser coherence length. For the experiment dealt with here, Fig. 1, the laser used has a coherence length of 50 mm, so the first to the second reference object beam pair optical path difference was chosen to be 80 mm, and 150 mm for first and third pair. With this point taken, the total intensity on the CCD sensor is the sum of the three independent intensities due to the reference object beam pairs,

$$I(\xi,\eta) = \sum_{k=1}^{3} I_k(\xi,\eta)$$
$$= \sum_{k=1}^{3} \left[\left| R_k(\xi,\eta) + O_k(\xi,\eta) \right|^2 \right] \quad (1)$$

where,

$$O_k(\xi,\eta) = o_k(\xi,\eta)\exp[i\phi_k(\xi,\eta)] \quad (2)$$

and

$$R_k(\xi,\eta) = r_k(\xi,\eta)\exp\left[-2\pi i\left(f_{k\xi}\xi + f_{k\eta}\eta\right)\right] \quad (3)$$

are the complex object and reference beam amplitudes, respectively. ξ and η are rectangular coordinates at the CCD detector plane. $f_{k\xi}$ and $f_{k\eta}$ represent spatial frequency carriers along directions ξ and η, due to a small inclination of each diverging reference beam with respect to the system optical axis z, see Fig. 1. Upon substitution of Eq. (2) and Eq. (3) into 1,

$$I(\xi,\eta) = \sum_{k=1}^{3} \{a_k(\xi,\eta)$$
$$+ c_k(\xi,\eta)\exp\left[2\pi i\left(f_{k\xi}\xi + f_{k\eta}\eta\right)\right]$$
$$+ c_k^*(\xi,\eta)\exp\left[-2\pi i\left(f_{k\xi}\xi + f_{k\eta}\eta\right)\right]\} \quad (4)$$

with,

$$a_k(\xi,\eta) = o_k{}^2(\xi,\eta) + r_k{}^2(\xi,\eta) \quad (5)$$

and

$$c_k(\xi,\eta) = o_k(\xi,\eta)r_k(\xi,\eta)\exp[i\phi_k(\xi,\eta)] \quad (6)$$

Either of the last two terms of Eq. (4), represent an interferogram with carrier spatial frequency $f_{k\xi}$ and $f_{k\eta}$, and phase modulated by $\varphi_k(\xi,\eta)$. As is commonly done in digital holography in order to recover the phase term $\varphi_k(\xi,\eta)$ a Fourier transform must be performed on Eq. (4),

#9861 - $15.00 USD
Received 5 December 2005; revised 30 January 2006; accepted 1 February 2006

$$FT\{I\} = \sum_{k=1}^{2} [A_k(f_\xi, f_n) + C_k(f_\xi - f_{k\xi}, f_n - f_{kn}) + C_k^*(f_\xi - f_{k\xi}, f_n - f_{kn})] \quad (7)$$

where capital letters correspond to the Fourier transform. The required phase term $\varphi_k(\xi,\eta)$ is contained in either of the complex conjugate terms C_k and C^*_k. For the 3D evaluation proposed here, there are six of these terms spatially separated at the Fourier spectrum plane. In digital holography this terms are spatially separated by the proper choice of shape and size of the aperture located in between the reference object beam combiner cube and the edge of the endoscope opposite to the object. Figure 2 shows the absolute value of the Fourier transform, i.e., the Fourier spectrum, for the simultaneous acquisition of the three pulsed digital holograms. Each pair of complex conjugate terms C_k and C^*_k may be easily identified for each reference object beam pair, as they are symmetrically located about $(f_\xi, f_\eta)=0$. Only three of these terms are filtered, each belonging to a reference object beam pair, and their inverse Fourier transform calculated in order to obtain the corresponding phase distribution

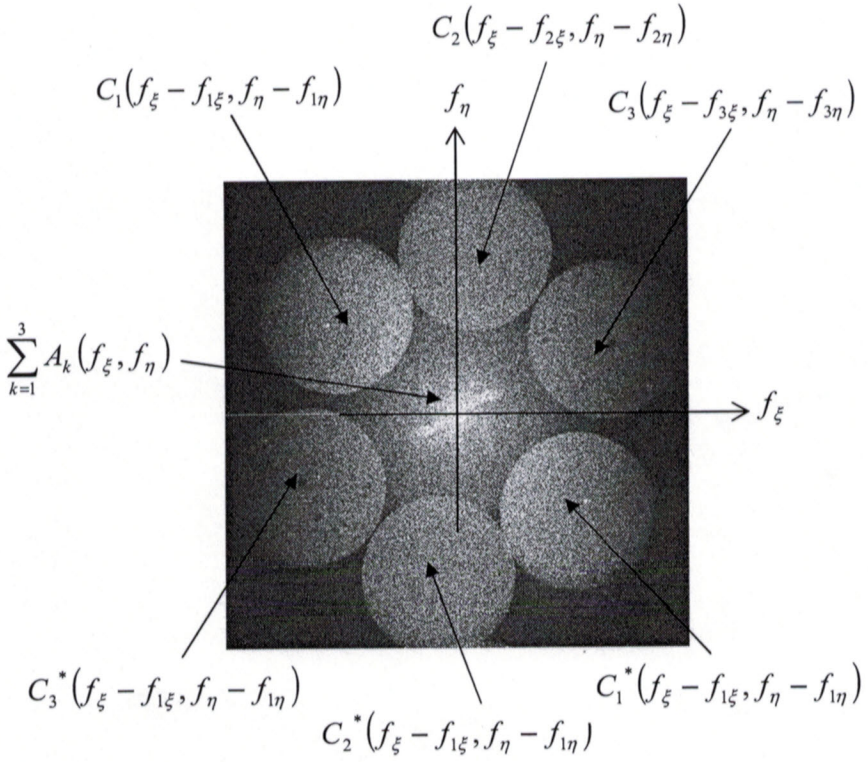

Fig. 2. Fourier spectrum consisting of three incoherently added digital holograms.

#9861 - $15.00 USD
Received 5 December 2005; revised 30 January 2006; accepted 1 February 2006

$$\phi_k(\xi,\eta) = \arctan\frac{\mathrm{Im}[c_k(\xi,\eta)]}{\mathrm{Re}[c_k(\xi,\eta)]}, \quad k = 1,2,3 \tag{8}$$

This procedure is done for the object at a certain position and for a single laser pulse. The next laser pulse captures the object at another position and the phase, viz., $\phi_k^{'}(\xi,\eta)$, is again extracted from each reference object beam pair obtained on a single CCD frame. Subtraction of the phase distribution obtained from each object position gives,

$$\Delta\phi_k(\xi,\eta) = \phi_k^{'}(\xi,\eta) - \phi_k(\xi,\eta), \quad k = 1,2,3 \tag{9}$$

This phase difference $\Delta\phi_k$ is then related to the sensitivity vector, $\vec{s}_k$, along each object illumination direction and the object displacement vector, $\vec{u}$, through the dot product,

$$\Delta\phi_k = \left(\frac{2\pi}{\lambda}\right)\vec{u}\cdot\vec{s}_k \tag{10}$$

where

$$\vec{s}_k = \hat{n}_k - \hat{n}_o, \qquad k = 1,2,3 \tag{11}$$

$\hat{n}_k$ y $\hat{n}_o$ are unitary vectors along the direction of object illumination and observation, respectively. For the experiment in hand, it is assumed that the orthogonal coordinate system origin is on the geometrical object center, (see Fig. 3). Eq. (10) allows the combination of the individual phases and sensitivity vectors, all data obtained from the experiment. The only remaining unknown is $\vec{u}$, the displacement vector along the *x*, *y* and *z* axes.

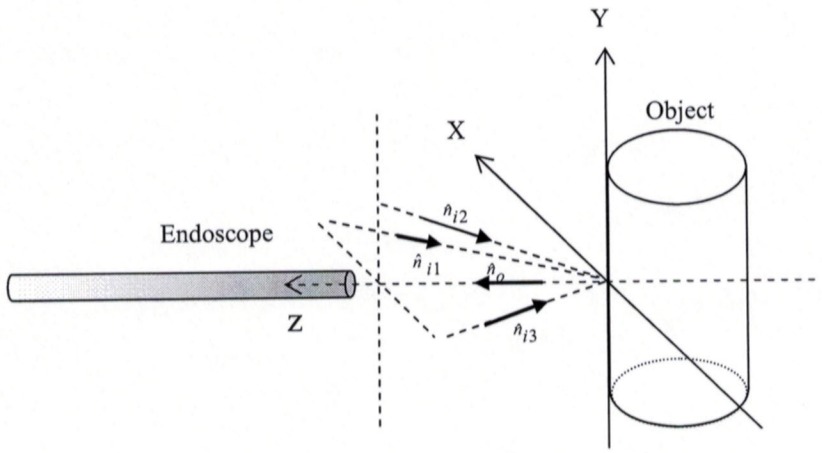

Fig. 3. Geometry of the illuminating beams, showing the unitary vectors of illumination.

3. **Results and discussion**

The experimental set up is shown in Fig. 1. A rigid endoscope made out of a lens system is used as the imaging system. The high resolution CCD sensor receiving the image, PULNIX TM-1001, has 1024X1024, pixel elements, with an area of $\Delta x \times \Delta x = 9\mu m^2$, each. The endoscope has the ability to form object images from 3 mm to 12 mm diameter: for this experiment the object area imaged is 12 mm. The separation from the endoscope edge to the object surface may be varied from 5 mm to 25 mm: 25 mm for this experiment. Pulses from a Nd:YAG laser emitting at 532ηm are divided initially into two beams, one that serves as

#9861 - $15.00 USD
Received 5 December 2005; revised 30 January 2006; accepted 1 February 2006

reference and the other as object. Each beam is further divided into three reference and object beams by means of beam splitters.

Each object beam is made to converge with a lens into a multimode optical fiber, and the lens-fiber set is attached to a sliding mechanical component that is later used to adjust the optical path length, like the one introduced by the distance from the endoscope edge to the object surface. The remaining part of the fiber length is attached to the endoscope so that all three object beams illuminate the surface area from three different positions by means of a mechanical support at the end of each fiber. With the latter the object is illuminated from three different directions at an angle α with respect to the z optical axis. This is the manner in which the unitary vectors of illumination $\hat{n}_k$ are defined. Finally, the three reference beams are sent to the CCD sensor using single mode optical fibers. The diverging beams have a relative inclination with respect to the z optical axis, and therefore to their respective object beam pair, of approximately 1.5°. This is done in order to physically separate the individual reference object beam pair Fourier components.

The object used was a metallic cylinder of 13 mm diameter, 19 mm height and 0.3 mm width. The cylinder is tightly fixed to a mechanical support so that the imaginary origin of the rectangular coordinate system rests always on its center. The cylinder is harmonically excited using a mechanical shaker on a point perpendicular to the optical axis. The excitation frequencies are scanned so the resonant modes are identified and one is chosen at 2180 Hz, with the laser pulses fired at a separation of 80μs, so that two object positions are acquired during a vibration cycle. As explained earlier, each pulse captures three incoherent digital holograms and their individual phase difference $\Delta\varphi_k$ is obtained by simply subtracting the phase information from one pulse to the other, i.e., the displacement information $\vec{u}$ may now be calculated from Eq. (10).

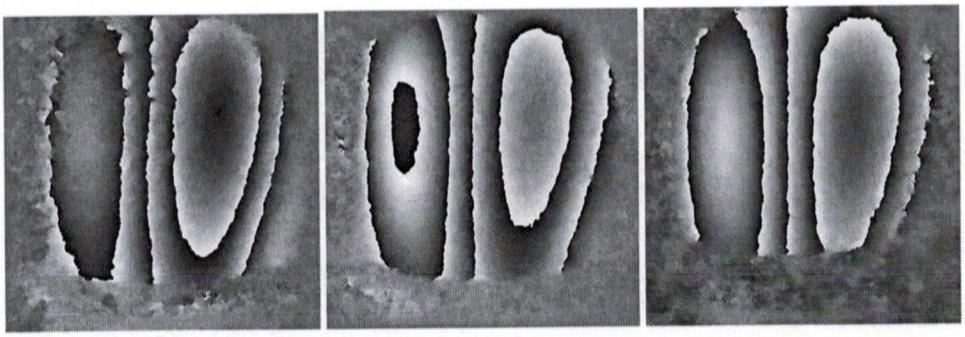

(a) (b) (c)

Figs. 4. (a), (b) and (c) are wrapped phase map of three illumination directions, $\hat{n}_{i1}$, $\hat{n}_{i2}$ and $\hat{n}_{i3}$ respectively.

Figure 4 shows the wrapped phase maps $\Delta\varphi_k$ for each reference object beam pair, i.e., for every object illumination direction. In order to work with Eq. (10), these phase maps need to be unwrapped so that the 2π discontinuities are taken into consideration. The object image has a diameter of 11mm, and from it only a reduced area (10mm x 9.5mm) is used to unwrap the phase maps. The sensitivity vector is then calculated by measuring the distances, from the origin, to the three object illumination sources and to the CCD sensor center. Once this is done it is possible to calculate $\vec{u}$, and indeed to separate independently of each other all three components of the deformation x, y and z. Figure 5 shows the normal, to the surface, displacement component drawn on a computer generated cylinder shape. Figure 6 shows the

#9861 - $15.00 USD Received 5 December 2005; revised 30 January 2006; accepted 1 February 2006

tangent displacement on the cylinder surface, with the arrows indicating the way in which the cylinder is deforming.

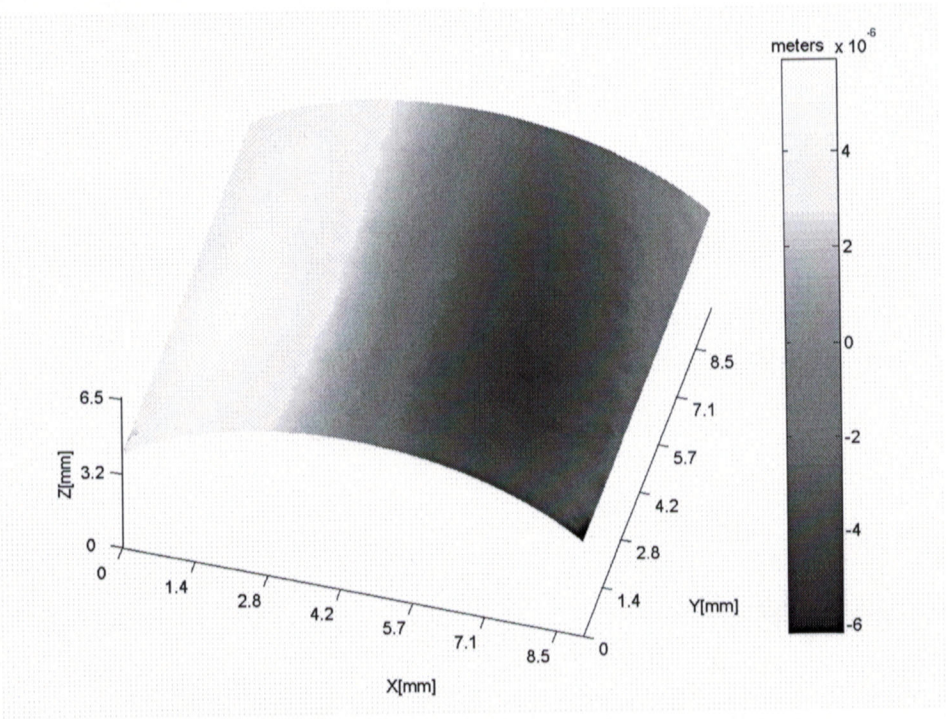

Fig. 5. The component of the resultant deformation normal to the cylinder surface.

#9861 - $15.00 USD
Received 5 December 2005; revised 30 January 2006; accepted 1 February 2006

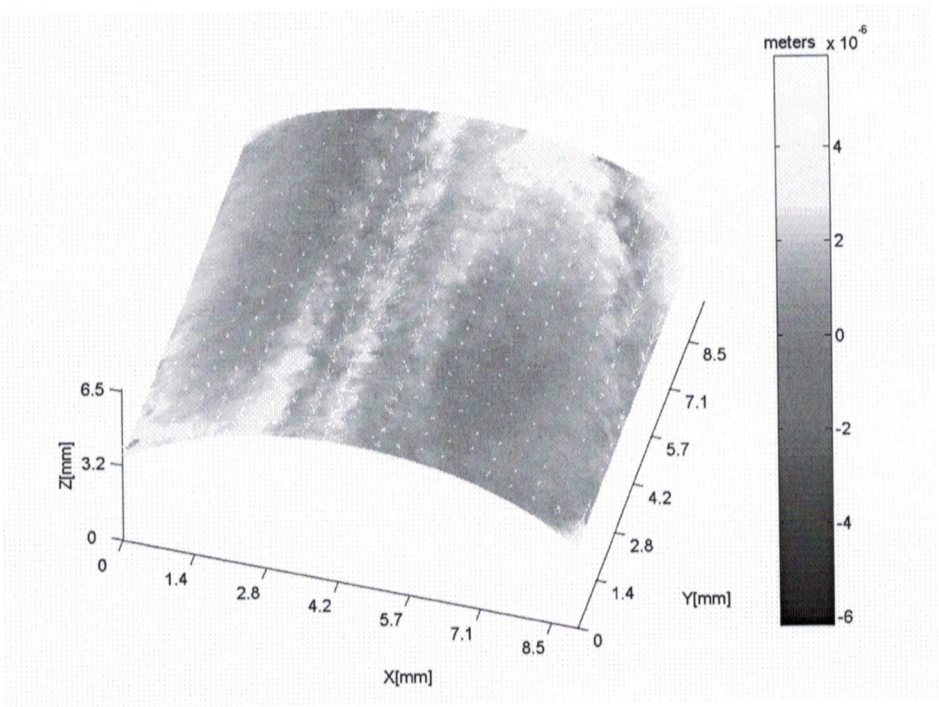

Fig. 6. The component of the resultant deformation tangent to the cylinder surface.

This endoscopic pulsed digital holography system has a drawback in that it uses a rigid endoscope so it is only possible to gain access in straight line to hidden object areas. The flexible endoscopes however, present a limited number of fiber that decrease, in comparison, the image quality of the object and thus bring a certain amount of information loss. Recently, miniaturized image plane digital holography interferometric systems were developed to record out-of-plane displacements[9], and 3D recording of Fresnel holograms in a sequential form[10]. The latter uses a set of robotic arms that allow access to very small apertures on the object, and once inside the arms open to allow object illumination from three different positions. This is a mechanical feature that is being considered for future work.

5. **Conclusions**

It was shown that the introduction of rigid endoscopes in conjunction with three object illumination using multi mode fiber sources into pulsed digital holography gives the opportunity to access and measure 3D displacements simultaneously from areas hidden within objects. This optical set up allowed the independent separation of the x, y and z displacements that may be further combined to obtain such data as the tangential and normal displacement to the object surface. Results for one of the metallic cylinder resonant modes was presented employing a pulse to pulse separation of 80μs, a time lapse set by the laser and CCD electronics. It is envisaged that this time can be decreased with the use of a twin cavity pulsed laser and a fast shutter CCD high resolution camera.

Acknowledgments

The authors would like to acknowledge partial financial support from CONACYT (Consejo Nacional de Ciencia y Tecnología, México) through project 42971, and the Landesstiftung Baden-Wurttemberg (Germany).

#9861 - $15.00 USD
Received 5 December 2005; revised 30 January 2006; accepted 1 February 2006